MODELING THE EFFECT OF WATER SPRAY SUPPRESSION ON LARGE-SCALE POOL FIRES

P. E. DesJardin, L A. Gritzo, and S. R. Tieszen
Sandia National Laboratories

ABSTRACT

In practical fire suppression systems for large rooms or compartments, water sprinklers are often located on or near the ceilings. In this configuration, the droplets from the water spray must be large enough to penetrate the high temperature thermal plume **of** the tire and reach the pool surface, yet be small enough to evaporate and provide effective suppression of the flame zone. The focus of this research is to investigate computationally the influence of initial drop size and spray system configuration on water suppression of medium to large scale (i.e., ~100kW) pool fires. The cases addressed are representative of ongoing experiments at the Naval Research Laboratories. The tire scenario examined in this study involves a 123kW heptane pool fire located in a 3.05m (10 ft) cube enclosed facility. Results from this study indicate that (1) for large drops ($D_d > 150\mu m$) an initial rise in temperature is observed associated with enhanced turbulent mixing before evaporative cooling takes place; (2) an optimum drop size is found that allows for maximum decrease in gas-phase temperature for one **of** the spray configurations examined: and (3) **a** low pressure spray with more nozzle locations appears to provide improved suppression when compared *to* using a single high pressure nozzle.

INTRODUCTION

The purpose of this research is to explore the use of numerical modeling for simulation of fire suppression using water sprays. This capability is useful to assess the performance of halon alternatives as driven by the ban on halon production. One attractive alternative for halon **is** the use of water sprays. The main physical mechanisms for flame suppression using water sprays include the effects of thermal cooling due to evaporation and gas phase heat capacity, oxygen displacement, and radiation attenuation due to the liquid spray.

A partial summary of the research in the use of water sprays for fire suppression can be found in the reviews by Tatem et al. [1], Jones et al. [2], Mawhinney et al. [3], and Grant et al. [4]. More recent numerical studies in this area can be found in the works of Chow et al. [5], Novozhilov et al. [6], and Prasad et al. [7, 8, 9]. Numerical suppression studies of Prasad et al. focused on the optimization of water sprays for the suppression of low Reynolds number (i.e., laminar) jet diffusion flames [7, 8] and pool fires [9]. The results of these studies demonstrate that suppression efficiency is highly dependent on the size of the water spray droplets as well as the location of the injection. Optimal suppression was observed when small drops are injected upward through the base of the flame. These conclusions are also supported in the work of Novozhilov et al. [6] and Chow et al. *[5]* for enclosure fires.

Novozhilov et al. [6] show reasonable agreement with experimental data by only considering the thermal effects of the spray, thus indicating that the chemical effects of water vapor on exothermic reaction kinetics are not significant. Lentati et al. [10] support this idea in their study examining the thermal and chemical suppression effects of water spray in a counter flow diffusion flame. Their results also indicate that the chemical suppression effects of water vapor contribute little (less then 10%) to the overall temperature drop indicating that thermal cooling due to evaporation of the water spray accounts for the majority of the suppression.

The complete understanding of water spray suppression of a turbulent fire involves resolving the intimate coupling of liquid evaporation, turbulence, finite rate chemical kinetics, and radiation heat transfer. The objective of this work is to account directly for the first three of these physical processes through subgrid modeling of pool fires for a scenario of engineering interest.

A detailed description of the subgrid models developed to account for thermal cooling (spray submodel) and chemical kinetics effects (PSR submodel) is provided in the Mathematical Model Formulation section. Results are then presented for a square (0.305 m [12 in]) 123 kW heptane pan fire, which is representative of tests at the Naval Research Laboratory (NRL) [11].* Numerical predictions are presented to examine the sensitivity of volume averaged temperature in the test cell to initial drop size specification and suppression system configuration.

MATHEMATICAL MODEL FORMULATION

The following mathematical description is limited to a summary of the spray and flame extinguishment model formulations used to account for the thermal and chemical effects of a liquid suppressant. respectively. The models are implemented into a general purpose fire simulation code, VULCAN. which is based on the KAMELEON-Fire code [12]. VULCAN uses a RANS based model suite including a k-ε turbulence model [13], the EDC combustion model [14], a soot model [15], and a radiation model [16]. The gas phase conservation equations are discretized on a staggered, block-structured grid with second-order upwind differencing for the convective terms using a version of the SIMPLE algorithm [17]. Previous studies using VULCAN for pool fire simulations can be found in references [18, 19, 20].

SPRAY SUBMODEL

The spray submodel is based on a stochastic separated flow approach [21]. The following transport equations for mass, momentum, and energy are integrated in time for groups of droplets (parcels).

$$\frac{dm_d}{dt} = \pi D_d \rho_f \frac{\nu_f}{Sc_f} B_m Sh_f$$

$$m_d \frac{du_{d_i}}{dt} = \frac{1}{8} \rho_g D_d^2 C_D \left| u_{g_i} - u_{d_i} \right| \left(u_{g_j} - u_{d_j} \right) + g m_d \delta_{3j} \qquad (1)$$

$$m_d C_d \frac{dT_d}{dt} = \pi D_d \rho_f \frac{\nu_f}{C_{p_f}} \mathrm{Pr}_f \left(T_g - T_d \right) Nu_f - \dot{m}_d h_{lg}$$

In Eq. (1), the Sherwood ($Sh_f = h_{m_d} D_d / D_{m_f}$) and Nusselt ($Nu_f = h_d D_d / k_f$) transfer numbers are expressed in terms of film conditions using the Ranz-Marshall correlations [22],

$$Sh_f = 2 \log(1 + B_m) / B_m \left[\mathrm{Re}_d^{1/2} Sc_f^{1/3} / 3 \right]$$
$$Nu_f = 2 \log(1 + B_m) / B_m \left[\mathrm{Re}_d^{1/2} \mathrm{Pr}_f^{1/3} / 3 \right] \qquad (2)$$

* Maranghides, A., Anleitner, R.L., Binnette, C., Austin, E.M. and Sheinson, R.S., *Results for Self-Contained Total Flooding Halon 1301 Alternative* Technologies *Evaluation*, NRL report. In progress, 2000, draft on file with the author.

The coefficient of drag (C_D) is modeled as that of a sphere using the relations from Shuen et al. [23],

$$C_D = \begin{cases} 24(1+\mathrm{Re}_d^{2/3}/6)/\mathrm{Re}_d & for\ \mathrm{Re}_d < 1000 \\ 0.44 & for\ \mathrm{Re}_d > 1000 \end{cases} \quad (3)$$

The thermodynamic properties at the droplet film surface are obtained by using a thin-skin approximation [21] where the film temperature is approximated as a weighted average of the droplet and surrounding gas temperatures, $T_f = \alpha T_g + (1-\alpha)T_d$. In this study, $\alpha = MIN(C_{Bi}\,Bi, 1)$ where $Bi\ (= h_d D_d / k_f)$ is the thermal Biot number. The model constant C_{Bi} (set equal to 0.5) defines the transition Bi number for which the droplet can be treated using a lumped capacitance approach (i.e., $T_d \cong$ T,). This model is used to account for rapid changes in droplet temperature as the droplet is transported into a flame zone. Attempts to use a simple 1/3 rule weighting [24] results in non-physical values of temperature and species mass fractions. The film is assumed to he at saturation conditions so that a partial pressure can be calculated using a Clausius-Clapeyron relation, $P_f = P_{ref} Exp\left[-h_{lg}/R\left(1/T_f - 1/T_{ref}\right)\right]$ where heat of vaporization, h_{lg}, is expressed as a function of temperature using Watson's relation [25, 26] (i.e., $h_{lg} = h_{lg_{ref}}\left[(T, - T_f)/(T_c - T_{ref})\right]^{0.38}$). Once the partial pressure is determined, the mass fraction of water vapor is calculated from the ideal equation of state, $Y, = MW_{H_2O}/MW_g\left(P_g/P_f - 1 + MW_{H_2O}/MW_g\right)$. Lastly, the mass ($B_m$) and thermal ($B_T$) transfer numbers in Eq. (1) are obtained from their definitions as derived from steady-state droplet analysis [27]: $B_m = (Y_g - Y_f)/(Y_f - 1)$ and $B_t = C_{P_f}(T_g - T,)/h_{lg}$.

Droplet dispersion due to turbulence is implemented using both parcel and subparcel models. The parcel model accounts for the effects of large-scale turbulent eddies perturbing a parcel trajectory and is based on the random walk model of Gosman and Ioannides [28] as modified by Shuen et al. [23]. Turbulent dispersion of the droplets within a parcel is accounted for using the group modeling concept of Zhou and Yao [29] where the spatial distribution of droplets within each parcel is assumed to have a Gaussian distribution.

FLAME EXTINGUISHMENT SUBMODEL

To account for the first order effects of the water spray on the exothermic chemical reactions in a flame, a subgrid model was developed based on Perfectly Stirred Reactor (PSR) theory as formulated by Glarborg et al. [30] in the CHEMKIN II [31] software package. The model is constructed through a sequence of PSR precalculations that map out chemical extinction time scales as a function of temperature and suppressant mixtures. For the current study, the suppressants include H_2O, CO_2, N_2, and combinations. In general, extinction times are functions of suppressant mixtures, temperature, and pressures and could be used in a tabulated lookup form. However, in order to reduce the storage requirements of such a table, mixing rules are used that allow the mixture mole fraction of suppressant to be determined using the following expression from Saito et al. [32]:

$$\frac{1}{X_{LIM_{mixture}}} = \sum_{species} \left(\frac{X_{relative}}{X_{LIM_{species}}} \right) \tag{4}$$

where $X_{LIM_{species}}$ is the suppressant mole fraction that extinguishes the flame for a specific suppressant species, $X_{relative}$ is the mole fraction of that particular suppressant species divided by the total suppressant mole fraction, and $X_{LIM_{mixture}}$ is the suppressant mole fraction for extinction for the suppressant in the specific fuel/air mixtures. These mixing rules only work for suppressants that are mostly thermal in nature [32] and so are well suited for studying the effects of water on flame suppression. An example of a chemical extinction time scale calculation is illustrated in Figures la and lb. These figures show the amount of N_2 and H_2O required for extinguishment of an H_2–air mixture as a function of residence time and temperature from the PSR-CHEMKIN calculations and representative curve fits. Mixtures of H_2O and N_2 are treated using the results of Figure 1 and the mixing rules of **Eq.** (4). The results show that, consistent with physical intuition, less suppressant is required to extinguish a flame with decreasing residence times ($t_{PSR_{blowout}}$) and more suppressant is required for extinguishment at higher temperatures. The VULCAN fire simulation package employs the PSR precalculations by assuming that the effective chemical time scale at the subgrid can be represented by a PSR *so* that $t_{chemical} = t_{PSR_{blowout}}$ and compares this time scale to a representative turbulence time scale at the subgrid, t_{flow}, which is estimated from classical turbulence theory, i.e., $t_{flow} = \sqrt{\nu / \varepsilon}$. If $t_{flow} < Da_{crit} t_{PSR}$, then blowout is assumed to occur and the reaction rates in the EDC combustion model are set equal to zero. The calibration parameter, Da_{crit}, for the model is the critical Damkohler number for extinguishment and is calibrated from jet blowoff studies* to a value of 1.367. **A** similar criteria for flame extinguishment has been recently used by Koutmos [33] for LES, but $Do_{,,,,}$ comes from a dynamic length scale ratio rather than an assumed constant. More details on the PSR flame extinction model forinulation and its calibration can he found in the reference of Tieszen and Lopez.*

NUMERICAL IMPLEMENTATION

The droplet transport equations of Eq. (1) are numerically integrated using the LSODE package for solving systems of stiff ODEs [34]. Gas phase properties needed for the evaluation of droplet transport processes are determined using linear interpolation from the Eulerian grid of the CFD calculations. As a first step, droplets that impact any wall of the computational domain before evaporating are simply removed from the calculation allowing a rather conservative prediction of suppression (i.e., dilution of the liquid fuel due to water spray is not modeled). The effects of the spray are coupled to the gas phase equations through appropriate source terms in the gas phase transport. The source terms are integrated into the gas phase transport equations using a dynamic time-splitting subcycling procedure similar to Amsden [35] to provide numerically stable solutions for rapidly evaporating sprays.

* Tieszen, **S.R.,** and Lopez, A., "Development of a Subgrid Fire Extinguishment Model," Technical report. Sandia National Laboratories, Albuquerque, NM. In final preparation, 2000. Draft on file with the author.

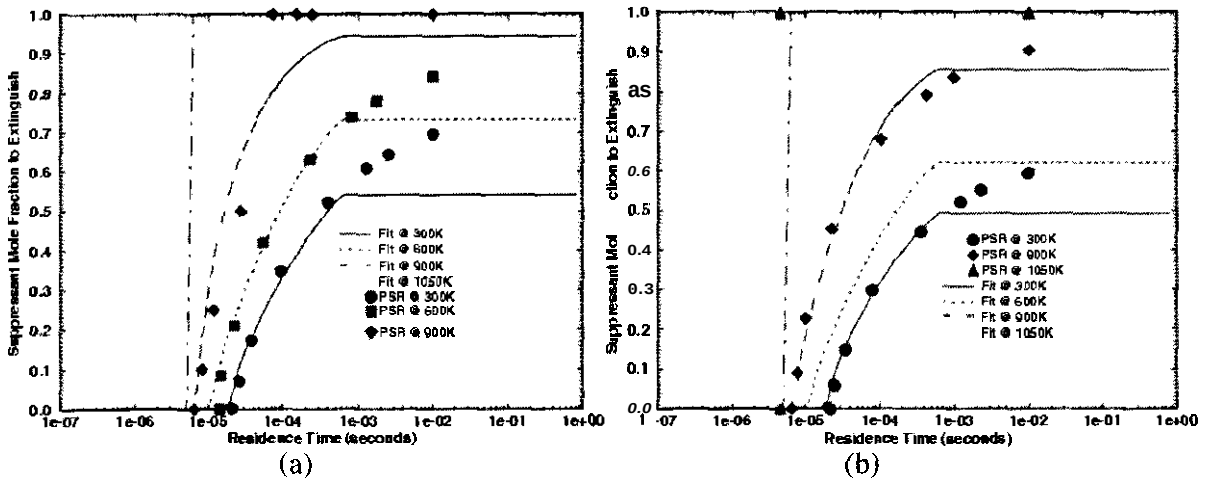

Figure 1. Blowout suppressant mole fraction vs. residence time for stoichiometric H_2/air mixtures with (a) N_2 (in excess of air) and (b) H_2O suppressants at 1 atm pressure. Symbols are from PSR-CHEMKIN calculations and lines are curve fits.

The VULCAN simulations presented here employ a 34 x 30 x 37 grid to discretize a cubical enclosure with a length of 3.05 m (10 ft) on a side. The simulations are first performed for 8600 time steps to simulate 45 sec of physical time to account for a typical prebum time for a fire to ignite and develop. The calculations are then advanced another 3500 time steps to allow for simulation of 10 sec of physical time to elapse with the water suppression activated. During the transient period of spray injection, a total of 33,000 computational parcels are injected into the domain with approximately 2000 parcels at any given time in the simulation.

RESULTS

A sketch of the NRL test facility is shown in Figure 2. The facility is ventilated using one inlet port located near the top of the enclosure and two exit ports located on the opposite corner. The volumetic flow rate is maintained at 7.1 m^3/sec allowing for one air exchange every 4 min. **A** 0.305 m (12") square pool of heptane is simulated through constant mass flux boundary conditions at the bottom of the domain. The mass flux is chosen as $\dot{m}'' = 0.0288\, kg/m^2 - \text{sec}$ based on empirical correlations from Drysdale [36] (i.e., $\dot{m}'' = \dot{m}''_\infty (1 - \exp(-k\beta D))$ where for heptane $\dot{m}''_\infty = 0.101$ and $k\beta = 1.1$) resulting in a 123-kW fire. In attempt to reproduce conditions from existing experimental procedures at the facility, a constant mass flow condition is imposed on the inlet boundary while a constant pressure condition is used at the outflow boundaries. After 45 sec, a constant pressure condition is imposed on both the inlet and outlet boundaries to simulate deactivation of the ventilation system. Two spray configurations, representative of the systems currently employed at NRL, are considered in this study and are illustrated in Figure 3. The first consists of a single high-pressure spray nozzle located at the center top of the enclosure while the second uses four lower pressure nozzles that cover each quadrant of the cell. Unfortunately, the exact drop size and velocity distributions, as well as the spray distribution pattern, are not well known and could not be obtained from the system manufacturers. Based on estimates of the operating pressures and atomizer cross sectional areas, the same mass flow rate, 0.53 kg/sec, was determined for both systems and droplet velocities of 166 and 83 m/sec for Configurations 1 and 2, respectively were calculated. The spray injection is modeled as a solid cone spray that randomly injects computational parcels to cover the specified solid angle. The

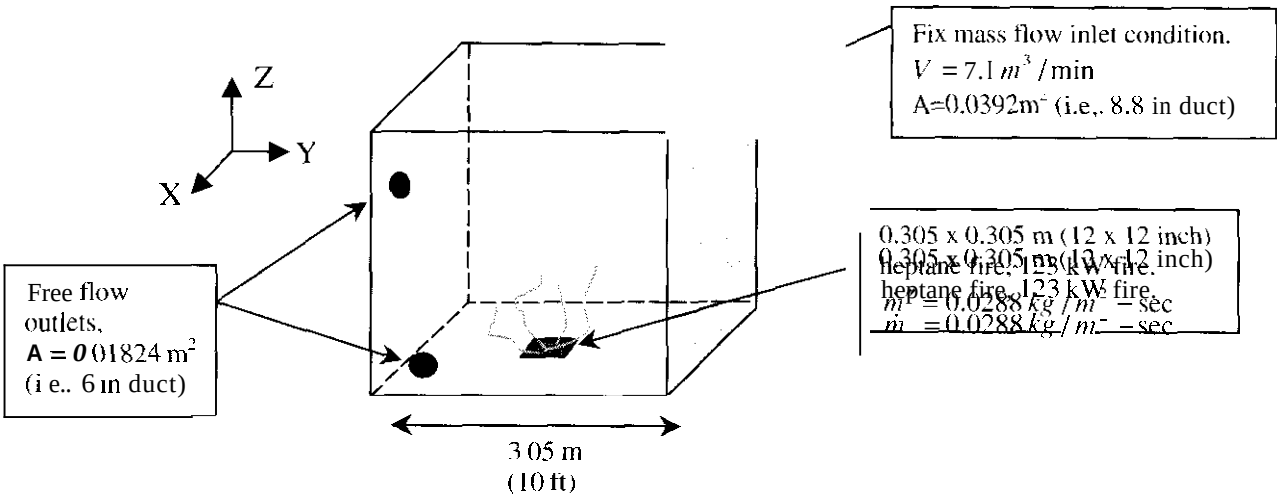

Figure 2. Schematic of NRL test facility.

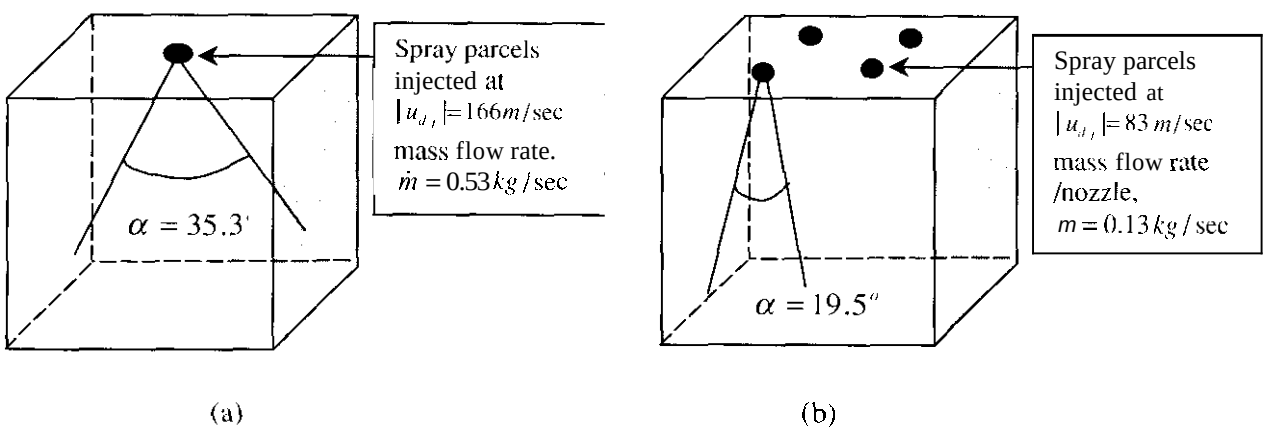

Figure 3. Schematic of spray system configurations using (a) one single high pressure nozzle (Configuration 1j and (b) quadrant approach using four lower pressure nozzles (Configuration 2).

spray angles (α) are computed to allow for a spray to reach the comers of the room in Configuration 1 or a cell quadrant in Configuration 2, if the droplet were to follow an outermost trajectory and are set equal to 35.3 and 19.5 deg, respectively. Lastly, four different drop size classes of D_d = 25.75, 150 and 300 μm are used for each configuration to explore the sensitivity of drop size and cover the range of plausible drop sizes expected in the experiments.

Figure 4a shows the volume averaged gas temperature for the lower half (i.e., Z < 1.5 m), <Tl>, upper half (i.e., Z > 1.5m), <Tu>, and for the entire domain, <T>, during the preburn part of the simulation. As shown, <Tu>, rapidly increases by approximately 100K in the first 30 sec of the preburn as the hot gases from the pool fire collect near the ceiling of the enclosure. After 30 sec, all temperature averages appear to increase approximately linearly at the same rate of 2 K/sec.

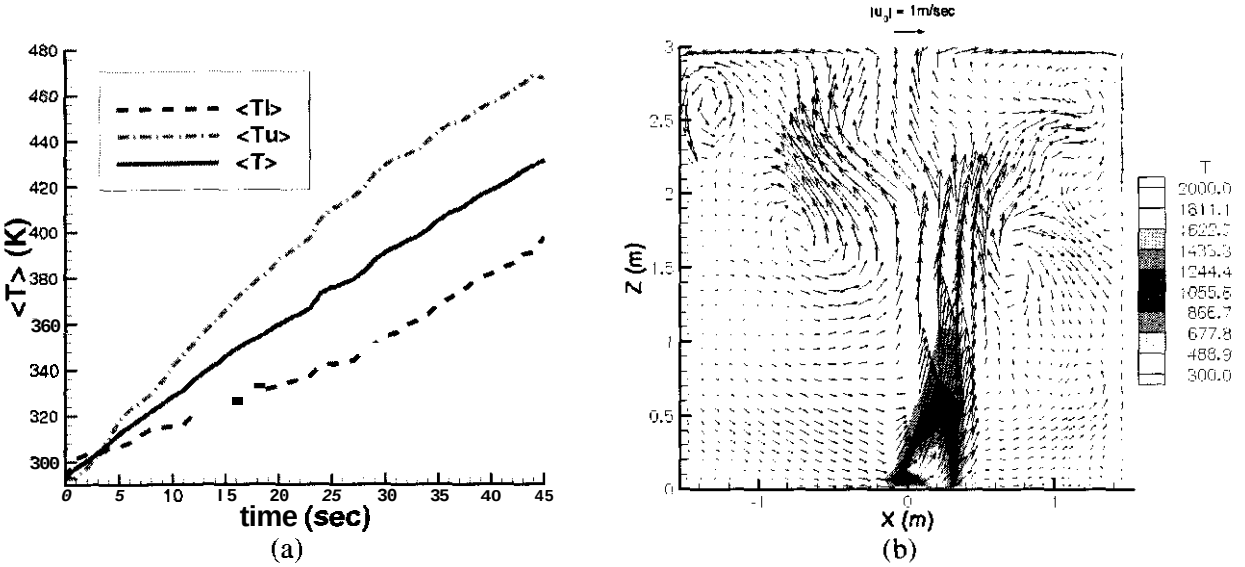

Figure 4. Temperature variations during preburn showing (a) volumetric average temperature versus time during prebum and (b) instantaneoous snapshot of temperature isocontour slice through center of cell (i.e., y=0) with superimposed velocity vectors after 45-sec prebum.

Figure 4b shows temperature isocontours with velocity vectors superimposed for a cross section through the domain after the preburn period. At this time, the flow shows large vortical flow structures that entrain air due to the periodic varicose puffing mode of the pool fire. In addition, the location of the peak temperature is shifted toward the outflow boundary resulting in the high temperature gases flowing on average along the ceiling to the exit boundary on the opposite wall.

After the prebum time, the water spray is injected forming a jet of entrained hot gas near the ceiling as the local air is transported by droplet drag and directed downward. Figure ***5*** shows instantaneous predictions of the gas phase velocity at the spray injection planes along with location and velocity of the droplets after 0.4 sec of spray injection using 150 μm droplets for (a) Configuration 1 and (b) Configuration 2. The maximum magnitude of the gas phase velocity for Configuration 2 is approximately 15 m/sec and is about half the peak value of 30 m/sec for Configuration 2. This difference is due to the lower mass flow and associated lower droplet injection velocities for the lower pressure four-nozzle system in Configuration 2.

Figure **6** presents volume averaged temperatures after the start of spray injection for Configuration 1 using all four drop size classes showing (a) <Tl> and (b) <Tu>. In Figure 6a, the largest, 300 μm, drops show an initial increase in temperature for the first 2.5 sec after injection. This surprising increase in temperature is due to the enhanced turbulent mixing of the jet and advection on the pool surface before enough water has evaporated to start to cool the flow near the base of the fire. This prediction is consistent with previous observations of Atreya et al. [37] on the use of water sprays. In contrast, the injection of the 25 μm drops results in a sudden drop of 40 **K** in the average temperature near the base of the fire in the first second, leveling off for another **3** sec and then suddenly decreasing again. This temperature history can be attributed to the transient jet development. A high concentration of small droplets are located at the leading edge of the jet offering effective suppression of the pool fire for a short (1 sec) period followed by enhanced turbulent mixing that slows the suppression until the initial jet transient has passed at 48 sec. The intermediate, 75 and 150 μm, cases also show signs of the transient jet develop-

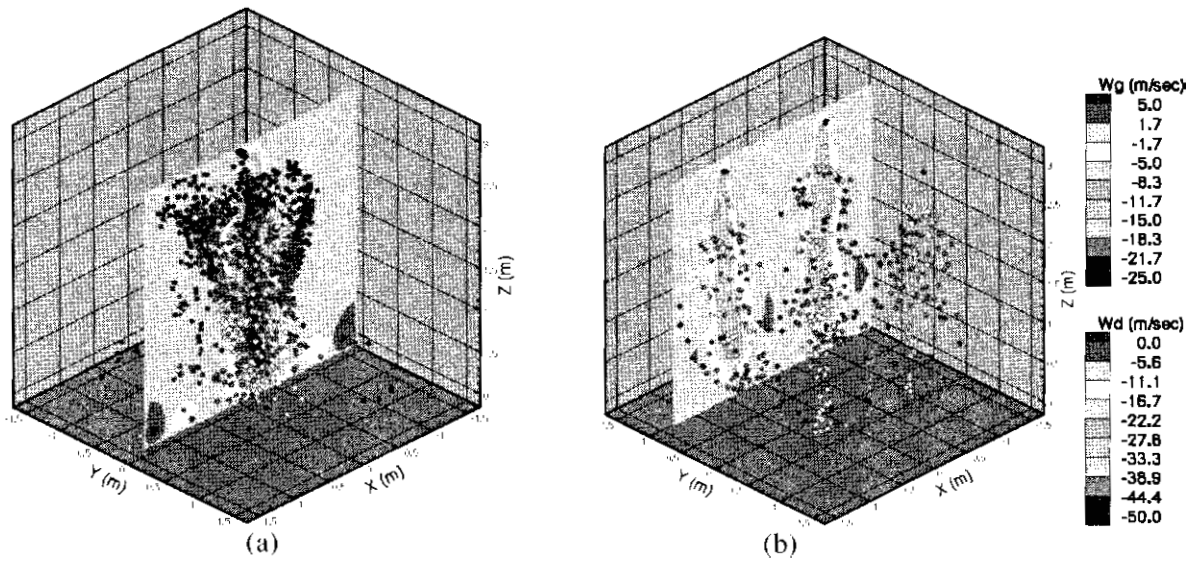

Figure 5. Instantaneous snapshot of water spray suppression 0.4 sec after injection showing isocontours of gas and droplet phase vertical velocity at plane of injection for (a) spray configuration 1 (contour slice at y=0.0 m) and (b) spray Configuration 2 (contour slice at y=-0.8 m).

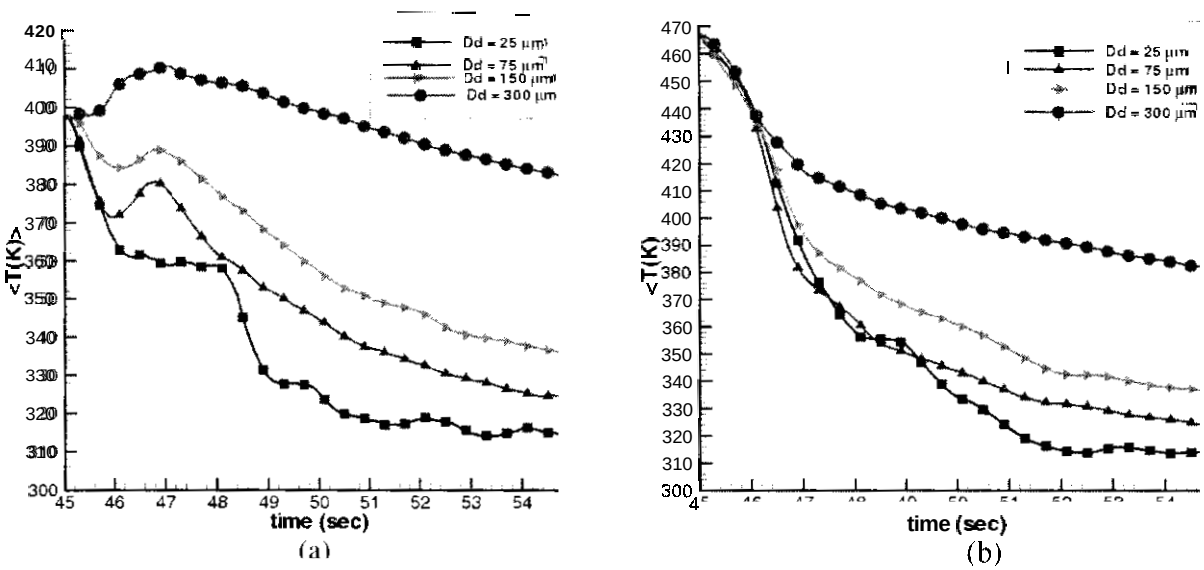

Figure 6. Volume averaged temperalure for Configuration 1 showing (a) <Tl> and (b) <Tu> verses time.

ment with some short-lived reduction in temperature due to initial injection of drops followed by an increase in temperature and then a more gradual decrease. Figure 6b shows <Tu> time history and indicates that, in general, the smaller droplets allow for more effective suppression than larger drops with the 25 and 75 µm providing almost same initial reduction in <Tu> for the first 4.5 sec after injection.

Figure 7 show (a) <Tl> and (b) <Tu> time history for the second spray system configuration. In this case, the enhanced turbulent mixing due to the startingjet from the sprays is not as pronounced as in Configuration 1 due to the lower injection velocities of the droplets and the spatial

offset of the spray injection locations relative to the position of the pool fire. The decrease in turbulent mixing, along with the longer residence time of droplets to interact with the fire, allows for the spray in Configuration *2* to decrease the <Tu> temperature more quickly than in configuration 1 as shown by comparing Figure 7b to 6b. In addition, Figures 7a and 7b indicate an optimum drop size exists between *25* and 75 μm that is sufficiently large to penetrate the high temperature fire plume, yet be small enough to be an effective suppressant at the flame zones. This observation is consistent with the previous water spray suppression studies of pool fires [4].

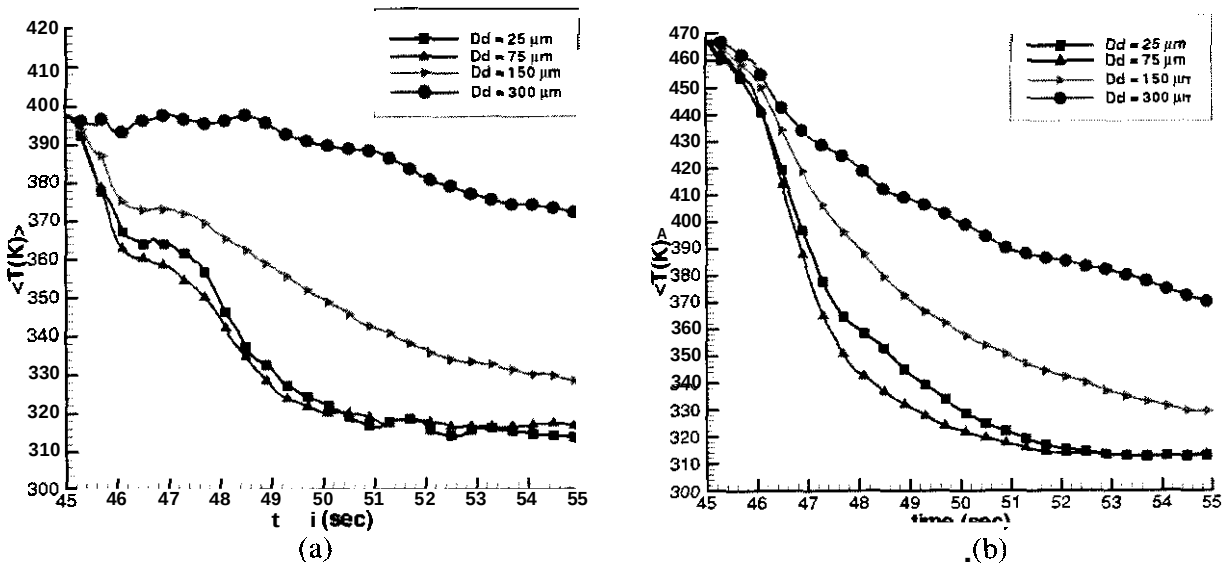

Figure 7. Volume averaged temperature for Configuration 2 showing (a) <Tl> and (b) <Tu> verses time.

CONCLUSIONS

In summary, a spray-suppression model applicable to simulating the effects of water mist on large-scale pool fires has been developed and applied to a practical fire scenario representative of experiments at NRL. The findings from this study indicate a strong sensitivity of fire suppression to initial drop size where injection of larger drops may actually cause an increase in overall temperature due to enhanced turbulent mixing before enough spray can evaporate to provide sufficient cooling. In spray Configuration 2, an optimum drop size was observed indicating that nozzles that generate very fine mist (i.e., $D_d < 50\ \mu m$) will not always provide maximum suppression for these conditions. Lastly, within the assumptions imposed for the inlet spray conditions and the fire scenario studied, the spray configuration using several lower pressure nozzles appeared to be slightly more effective at decreasing the gas phase temperature shortly after spray injection than a single high pressure nozzle.

ACKNOWLEDGMENTS

This work was supported in part by the US Department of Energy Defense Programs under the Engineering Sciences Research Foundation, the Department of Defense Safety and Survivability of Aircraft Initiative, and the Next-Generation Fire Suppression Program. This work was performed at Sandia National Laboratories, a multiprogram laboratory operated by Sandia Corporation, a Lockheed-Martin Company, for the US Department of Energy under contract DE-AC04-94AL85000.

REFERENCES

1. Tatem, P.A., Beyler. C.L., DiNenno, P.J., Budnick, E.K., Back, G.G., and Younis. S.E., "A Review of Water Mist Technology for Fire Suppression." Technical Report No. 94-33190, Naval Research Laboratory, Washington. DC, 1994.

2. Jones, A., and Nolan, P.F., "Discussions on the Use of Fine Water Sprays or Mists for Fire Suppression," *Loss Prev. Process Ind.*, 8, 17-22. 1995.

3. Mawhinney, J. R., and Richardson, J.K.. "A Review of Water Mist Fire Suppression Research and Development, 1996," *Fire Technology First Quarter 1997*, 55-90, 1996

4. Grant, G., Brenton J., and Drysdale, D., "Fire Suppression by Water Sprays." *Prog. Energy Combust. Sci.*, 26, 79-130, 2000.

5. Chow, W. K., and Fong, N. K., "Application of Field Modeling Technique to Simulate Interaction of Sprinkler and Fire-Induced Smoke Layer." *Combust. Sci. and Tech.*, 89, 101-151, 1993.

6. Novozhilov. V., Moghtaderi, B., Fletcher, D.F., and Kent, J.H., "Numerical Simulation of Enclosed Gas Fire Extinguishment by a Water Spray,"./. *Applied Firr Science*, 5, 135-146, 1996.

7. Prasad, K., Li. C.. and Kailasanath, K., "Optimizing Water-Mist Injection Characteristics for Suppression of Coflow Diffusion Flames." In *Proceedings of 27th Symp. (Int.) on Combustion*," The Combustion Institute, Pittsburgh, PA., pp. 2847-2855, 1998

8. Prasad, K.. Li, C., Kailasanath, K., Ndubizu, C., Gopal, R., and Tatem, P., "Numerical Modeling of Water Mist Suppression of Methane-Air Diffusion Flame," *Combust. Sci. and Tech.*, 132, pp. 325-364, 1998

9. Prasad, K., Li, C., and Kailasanath, K.. "Simulation of Water Mist Suppression of Small Scale Methanol Liquid Pool Fires," *Fire Safety Journal*, *33*, pp. 185-212. 1999.

10. Lentati. A.M.. and Chelliah, H.K., "Physical, Thermal and Chemical Effects of Fine-Water Droplets in Extinguishing Counterflow Diffusion Flames." In *Proceedings ofthe 27'" Symp. (Int.) on Combustion*, The Combustion Institute, Pittsburgh, PA, pp. 2839-2846, 1998.

11. Black, B.H., Maranghides, A., Sheinson, R.S., and Darwin, R., "Flanimable Liquid Storeroom Halon 1301 Replacement Testing—Phase 1: Testbed Design and Instrumentation." *Proceedings*, Halon Options Technical Working Conference. Albuquerque, NM, pp. 343-354, 1997.

12. Holen, J., Brostøm, M., and Magnussen, B.F., "Finite Difference Calculation of Pool Fires," In *Proceedings of 23rd Symp. (Int.) on Combustion*, The Combustion Institute, Pittsburgh, PA, pp. 1677-1683, 1990.

13. Jones, W.P., and Launder, B.E., "The Predicrion of Laminarization With a Two-Equation Model of Turbulence," *Int. ./. Heat Mass Transfer*, 15, pp. 301-314, 1972.

14. Byggstøyl, S., and Magnussen. B.F., "A Model for Flame Extinction in Turbulent Flow," *In Proceedings of 17th Sump. (Int.) on Combustion*, The Combustion Institute, Pittsburgh, PA, pp. 381-395, 1978.

15. Magnussen, B.F., *Particle Carbon Formation During Combustion*, Plenum Publishing Corp., 1981.

16. Lockwood, F.C., and Shah, N.G., "A New Radiation Solution Method for Incorporation in General Combustion Prediction Procedures," In *Proceedings of 18th Symp. (Int.) on Combustion,* The Combustion Institute, Pittsburgh, PA, pp. 1405-1414, 1981.

17. Patankar, S.V., *Numerical Heat Transfer and Fluid Flow,* Hemisphere Publishing Co, New York, NY, 1980.

18. Gritzo, L.A., Nicolette, V.F., Tieszen, S.R., Moya, J.L., and Holen, J., "Heat Transfer to the Fuel Surface in Large Pool Fires," In Chan, **S.H.,** editor, *Transport Phenomena in Combustion,* Taylor & Francis, pp. 701-712, 1995.

19. Tieszen, S.R., Nicolette, V.F., Gritzo, L.A., Holen, J., Murray, D., and Moya, J.L., *Vortical Structures in Pool Fires: Observation, Speculation, and Simulation,* Technical Report SAND96-2607, Sandia National Laboratories, Albuquerque, NM, 1996.

20. Gritzo, L.A., and Nicolette, V.F., "Coupling of Large Fire Phenomenon with Object Geometry and Object Thermal Response," *Journal of Fire Sciences,* 15, pp. 427-442, 1997.

21. Faeth, G.M., "Mixing, Transport and Combustion in Sprays," *Proy. Energy Combust. Sci.,* 13, pp. 293-345, 1987

22. Ranz, W. E., and Marshall, W.R., "Evaporation from Drops," *Chem. Engrg. Prog.,* 48, pp. 141-173, 1952.

23. Shuen, J-S., Chen, L-D., and Faeth, G.M., "Evaluation of a Stochastic Model of Particle Dispersion in **a** Turbulent Round Jet," *AIChE Journal,* 29, pp. 167-170, 1983.

24. Crowe, **C.,** Sommerfeld, M., and Tsuji, Y., *Multiphase Flows with Droplets and Particles,* CRC Press, New York, NY, 1998.

25. Watson, K.M., "Prediction of Critical Temperatures and Heats of Vaporization," *Ind. Eng. Chem.,* 23, pp. 360-364, 1931.

26. Lefebvre, A.H., *Atomization and Sprays,* Hemisphere Publishing Corporation, New York, NY, 1989.

27. Sirignano, W.A., *Fluid Dynamics and Transport of Droplets and Sprays,* Cambridge University Press, Irvine, CA, 1999.

28. Gosman, A.D., and Ioannides, E., "Aspects of Computer Simulation of Liquid-Fueled Combustion," AIAA Paper 81-0323, 1981.

29. Zhou, Q., and Yao, S.C., "Group Modeling of Impacting Spray Dynamics," *Int. J. Heat Mass Transfer,* 35, pp. 121-129, 1992.

30. Glarborg, P., Kee, R.J., Grcar, J.F., and Miller, J., *PSR: A Fortran Program for Modeling Well Stirred Reactors,* Technical Report SAND85-8209, Sandia National Laboratories, Livennore, CA, 1986.

31. Kee, R.J., Rupley, F.M., and Miller, J.D., *CHEMKIN 11: A Fortran Chemical Kinetics Package for the Analysis of Gas-Phase Chemical Kinetics,* Technical Report SAND89-8009, Sandia National Laboratory, Livermore, CA, 1989.

32. Saito, N., Ogawa, Y., Saso, Y., Liao, C., and Sakei, R., "Flame-Extinguishment Concentrations and Peak Concentrations of N_2, AR, CO_2, and Their Mixtures for Hydrocarcon Fuels," *Fire Safety Journal,* pp. 185-200, 1999.

33. Koutmos, P., "Simulations of Turbulent Methane Diffusion Flames with Local Extinction Effects," *Fluid Dynamics Research*, 24, pp. 103-119, 1999.

34. Radhakrishnan, K., and Hindmarsh, A.C., *Description and Use of LSODE, the Livermore Solver for Ordinary Differential Equations*, Technical Report UCRL-ID-113855, Lawrence Livermore National Laboratory. Livermore, CA, 1993.

35. Amsden, A.A., Ramshaw, J.D., Cloutman. L.D., and O'Rourke, P.J., *Improvements and Extensions to the KIVA Computer Program*, Technical Report LA-10534-MS, Los Alamos National Laboratory, Los Alamos, NM, 1985.

36. Drysdale. D., *An Introduction to Fire Dynamics*, Second Edition, John Wiley & Sons, New York, NY, 1998.

37. Atreya, A., Crompton, T.. and Suh, J.. "An Experimental and Theoretical Study of Mechanisms of Fire Suppression by Water," NIST Report NISTIR 5499, 1994.